# Spectroscopic Properties of 2′-(or-3′)-*O*-(2,4,6-Trinitrophenyl) Adenosine 5′-Triphosphate Revealed by Time-Resolved Fluorescence Spectroscopy

**Jing Yong Ye,* Masayo Yamauchi, Osamu Yogi, and Mitsuru Ishikawa**

*Joint Research Center for Atom Technology (JRCAT), Angstrom Technology Partnership (ATP), National Institute for Advanced Interdisciplinary Research, 1-1-4 Higashi, Tsukuba, Ibaraki 305-0046, Japan*

*Received: October 23, 1998; In Final Form: January 28, 1999*

We examined the spectroscopic properties of a fluorescent nucleotide analogue, 2′-(or-3′)-*O*-(2,4,6-trinitrophenyl) adenosine 5′-triphosphate (TNP-ATP), using time-resolved fluorescence spectroscopy. Our study clearly shows that the change in fluorescence intensity of TNP-ATP with different solvent properties has disparate origins, which were obscured in previous steady-state measurements. The four main findings are as follows. First, the fluorescence lifetime of TNP-ATP was found to increase with increasing viscosity, resulting in an increase in quantum yield, and therefore, fluorescence intensity. Second, fluorescence intensity increased with increasing pH ranging from 2.4 to 8.1. However, the fluorescence lifetime was essentially independent of the change in pH. The change in fluorescence intensity was not due to variations in quantum yield, but to the change in absorbance with pH. Third, we examined the interaction of TNP-ATP with the Klenow fragment of DNA polymerase I and found that free TNP-ATP and bound TNP-ATP in two binding sites were distinguished by using time-resolved spectroscopy, although the binding site with lower affinity could not be resolved in previous steady-state measurements. As the enzyme concentration was increased, the fluorescence lifetime of the enzyme−TNP-ATP complex remained unchanged, but the fractional fluorescence intensity of the bound TNP-ATP increased, thus leading to an increase in total fluorescence photocounts. Last, the fluorescence of TNP-ATP in the presence of the enzyme was further enhanced by the addition of $Mg^{2+}$. This enhancement was due to the increase in the fractional fluorescence intensity of the bound TNP-ATP rather than to the change in fluorescence lifetime. This finding indicates that $Mg^{2+}$ raises the affinity of the enzyme for TNP-ATP.

## I. Introduction

A variety of ATP fluorescent analogues have been synthesized[1−4] to acquire information on ATP, which plays a crucial role in many biochemical processes. Among the various analogues, 2′-(or-3′)-*O*-(2,4,6-trinitrophenyl) adenosine 5′-triphosphate (TNP-ATP), has been widely used as substrates, inhibitors, and structure probes of a large number of proteins[5−14] because of its unique fluorescence properties and high binding affinity to proteins. Moreover, owing to its broad absorption spectrum being likely to overlap with donor emission spectra, TNP-ATP also acts as an acceptor in fluorescence resonance energy transfer.[15−20]

The ribose-modified fluorescent nucleotide analogue, TNP-ATP, contains a Meisenheimer complex moiety and has a fluorescence quantum yield as low as $2 \times 10^{-4}$ in an aqueous solution.[5,7] However, the fluorescence properties of TNP-ATP strongly depend on local environments; the fluorescence intensity increases with increasing viscosity or with decreasing solvent polarity[5,7] and is notably enhanced when TNP-ATP is bound to proteins.[5−14] Although many studies have taken advantage of this environment-sensitive nature by using TNP-ATP as a fluorescent probe, all of them were limited to steady-state fluorescence measurements. To date, time-resolved spectroscopic studies have not been reported. The extremely low fluorescence quantum yield and fast decay of TNP-ATP make it difficult to perform time-resolved fluorescence measurements. Thus, recent attempts by Lin and Faller to obtain the anisotropy decay of TNP-ATP were unsuccessful.[17] There is only a rough estimate of the fluorescence lifetime in ethanol (50 ps) made by Moczydlowski and Fortes with a steady-state anisotropy measurement.[7] On the other hand, just owing to the low quantum yield in the aqueous solution, there is a large margin for a change in fluorescence efficiency with local environments. While we previously demonstrated that fluorescent probes with a low quantum yield may be more sensitive to surroundings than fluorophores with higher quantum yields near unity,[21−23] this is not always the case. It is therefore noteworthy that the special fluorescence nature of TNP-ATP ensures its use as an extremely sensitive local probe.

Despite the wide applicability of TNP-ATP as a useful fluorescent nucleotide analogue, the dynamics of its fluorescence is still poorly understood. To understand the origins of the change in fluorescence intensity of TNP-ATP in different environments, it is important to investigate how the local environment influences the dynamics. In the present study, we used a time-resolved fluorescence measurement, because unlike a steady-state measurement, it can monitor the transient nature of fluorescence properties. We simultaneously measured the time-resolved fluorescence spectra and decay curves of TNP-ATP on two-dimensional images with an ultrafast laser system and a single photon-counting streak scope. This experiment revealed the transient fluorescence properties of TNP-ATP and indicated that different mechanisms are involved in the change in fluorescence intensity with viscosity (glycerol/water mixtures of various glycerol percentage), pH (2.4 to 8.1), and titrations

* To whom correspondence should be addressed. E-mail address: jyye@jrcat.or.jp.

10.1021/jp984232k CCC: $18.00 
Published on Web 03/20/1999

with an enzyme (the Klenow fragment of DNA polymerase I) and a metal ion ($Mg^{2+}$). Two binding sites of the Klenow fragment for TNP-ATP were distinguished with time-resolved spectroscopy. The binding site with lower affinity could not be resolved in previous steady-state measurements. Moreover, our experimental findings also revealed that $Mg^{2+}$ raises the affinity of the enzyme for TNP-ATP.

## II. Experimental Section

**Time-Resolved Fluorescence Measurements.** The laser system that we used was based on a mode-locked Ti:sapphire laser (Coherent, Mira 900F) pumped with a continuous wave (cw) argon ion laser (Coherent, Innova 425). The output pulses oscillating at a repetition rate of 76 MHz had a typical pulse width of 120 fs full width at half-maximum (fwhm) and were tuned to 800 nm in wavelength. An ultrafast harmonic generation system (Inrad, model 5−050) was used as a second harmonic generator to double the frequency of the ultrashort pulses from the Ti:sapphire laser. The 400-nm pulses were attenuated to ∼1 mW and focused on the sample. A Babinet-Soleil compensator was set at a quarter-wavelength of the excitation light, which changed vertically polarized to circularly polarized excitation to avoid the issue of reorientational relaxation of fluorophores. The emitted fluorescence collected at 90° to the excitation beam was collimated and focused on the entrance slit of a polychromator (Chromex, 250IS) after passing through a long-pass filter to remove the scattered light from the laser pulses. An astigmatism-corrected holographic grating (Chromex, 50 grooves/mm) with high efficiency in fluorescence collection was used in the polychromator, which allowed a wide spectral range of 286.5 nm to be covered in one measurement. The wavelength calibration was done with a low-pressure mercury lamp. The wavelength-resolved fluorescence from the polychromator further entered a single photon counting streak scope (Hamamatsu, C4334) to obtain time-resolved spectra.[24] The time resolution depends on the full time range chosen for the measurements, typically 22 ps fwhm for a 1-ns full time range and 195 ps fwhm for a 10-ns full time range. Simultaneous measurements of lifetimes and spectra are displayed as two-dimensional images, each of which is composed of 640 × 480 pixels, where each pixel is equivalent to a 16-bit photon counter. The channel number of 640 was assigned to the spectral range, while that of 480 was allotted to the time range. The entire instrumentation was housed in a clean-air booth (class 10000), and all the measurements were done at 23 °C.

**Absorbance Measurements.** The absorption spectra of TNP-ATP in glycerol/water mixtures of different glycerol percentage (55 to 99% v/v) and pH (2.4−8.1) were recorded on a double-beam spectrophotometer (Hitachi, U-2000A). However, limited by the small amount of the Klenow fragment, the absorption spectra of TNP-ATP when titrated with the enzyme could not be measured.

**Materials and Preparation of Samples.** The nucleotide analogue TNP-ATP that we used was purchased from Molecular Probes. The Klenow fragment of DNA polymerase I (Pol I) was a product of Stratagene Cloning Systems. Spectrophotometric grade glycerol and spectroscopically pure magnesium chloride hexahydrate were obtained from Aldrich. Tris−HCl was supplied by Wako.

TNP-ATP was dissolved in the mixtures of glycerol and 0.2 M Tris−HCl with various percentages of glycerol (v/v) ranging from 55 to 99%. The concentration of TNP-ATP was estimated to be 49 $\mu$M by using a molar extinction coefficient of 26 400 $M^{-1}$ $cm^{-1}$ at 408 nm for neutral and basic pH values.[5] The pH dependence of the spectroscopic properties of TNP-ATP was examined for a glycerol percentage (v/v) of 87% and a TNP-ATP concentration of 49 $\mu$M. The pH of the solution was adjusted from 8.1−2.4 by the addition of HCl. The sample was put into an 1-cm light-pass quartz cell for both the absorption and fluorescence measurements.

Titration of TNP-ATP with the Klenow fragment was done by first preparing concentrated samples of the enzyme (6.2 $\mu$M) mixed with 4.0-$\mu$M TNP-ATP in 0.2 M Tris−HCl and then diluting the enzyme solution by adding 4.0-$\mu$M TNP-ATP solutions without the enzyme to keep the TNP-ATP concentration at a constant level. Titration was done in a 2-mL plastic microcentrifuge tube, and then the well-mixed sample was put into a quartz capillary as a sample cuvette for the fluorescence measurements. The capillary (1-mm i.d. and 3-mm o.d.) had a polished surface to reduce the scattering of excitation light by surface irregularities.

## III. Results and Discussion

**Viscosity Dependence of the Spectroscopic Properties of TNP-ATP.** Changes in viscosity of the TNP-ATP solution were produced by adjusting the ratio between glycerol and water, where the viscosity of glycerol at room temperature is 1490 cP, much higher than that of water (1 cP). The absorption spectrum of TNP-ATP is independent of the ratio between glycerol and water. A representative absorption spectrum is shown in Figure 1a.

The time-resolved fluorescence measurements of TNP-ATP were carried out for different solvent compositions with various glycerol percentages (v/v) from 55 to 99%. Time-resolved fluorescence spectra for the 90% glycerol (v/v) solution (Figure 1b) show that the emission maximum of the fluorescence spectrum shifted to lower energy with time after excitation, from 545 nm in the initial decay to 565 nm for the long-time decay region. The time-dependent Stokes shift was extensively studied and attributed to the solvation process.[25−28] Upon excitation, the solute−solvent system undergoes a Franck−Condon transition to a state in which the solute dipole has its excited-state value while the solvent molecules still occupy their previous configuration. Thus the equilibrium of solvent with ground-state solute is broken. The solvent molecules then relax to a configuration of lower energy, which is in new equilibrium with the electronically excited solute. This process leads to a Stokes shift of the emission peak to a longer wavelength. The solvation in polar media was investigated by many researchers, such as Simon,[25] Fried, and Mukamel,[26] while observation of the solvation in a nonpolar solvent was first reported by Fourkas and Berg,[27] although the coupling of solute molecules with a nonpolar solvent is much smaller than that in a polar system. The solvation process also occurred in our sample and resulted in the observed time-dependent Stokes shift. In Figure 1b the steady-state fluorescence spectrum that may be considered as the time-integrated spectrum is also shown for comparison with the time-resolved spectra.

The fluorescence decay curve determined over the entire emission spectrum is a nonexponential shape, as shown in Figure 2. Because we used circularly polarized light to excite TNP-ATP molecules, thus causing the excited-state dipoles to be randomly distributed, the contribution of reorientational relaxation of the solute dipole to the decay curve was excluded. To focus our attention on the origin of the enhancement of fluorescence with increasing solvent viscosity, we examined the viscosity dependence of fluorescence lifetime. Here we only try to extract fluorescence lifetime from the decay curve by using

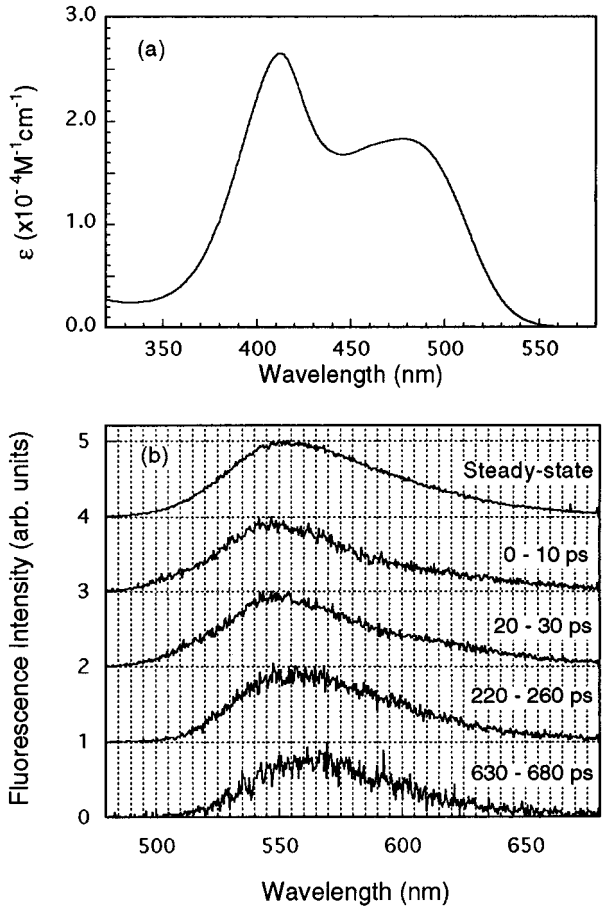


**Figure 1.** Absorption spectrum and fluorescence spectra of TNP-ATP in glycerol/water mixture. The percentage of glycerol (v/v) in 0.2 M Tris−HCl (pH 8.0) was 90%. (a) Absorption spectrum and (b) time-resolved fluorescence spectra of TNP-ATP excited by ultrashort laser pulses at 400 nm. The data accumulation time was 300 s. The steady-state spectrum is also included for comparison. All spectra were normalized to unity at their maximum and were shifted vertically by one unit with respect to each other.

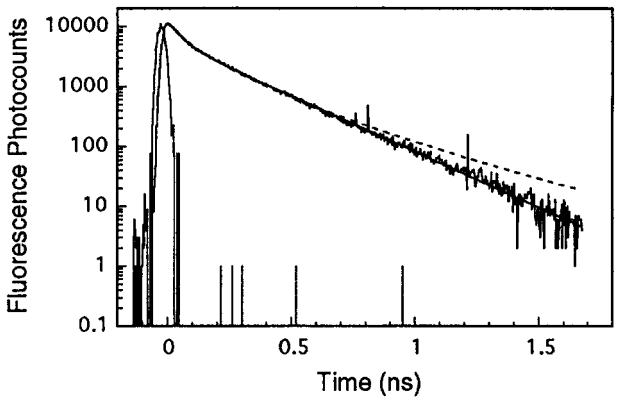


**Figure 2.** Fluorescence decay curve of TNP-ATP in a 90% (v/v) glycerol/water mixture. The instrument-response function with 22 ps fwhm is also plotted. The fitting process included deconvolution. The dashed line is the fit to a stretched exponential function, and the solid line is that to a biexponential function.

curve-fitting, and we will report on the detailed solvation dynamics elsewhere.

To fit the nonexponential decay curve, we tested two fitting functions. For a first trial, we fitted the data to a stretched exponential function, also known as the Kohlraush−Williams−Watts function,[27,29,30] which is frequently used to characterize a nonexponential decay with a distribution of time constants.

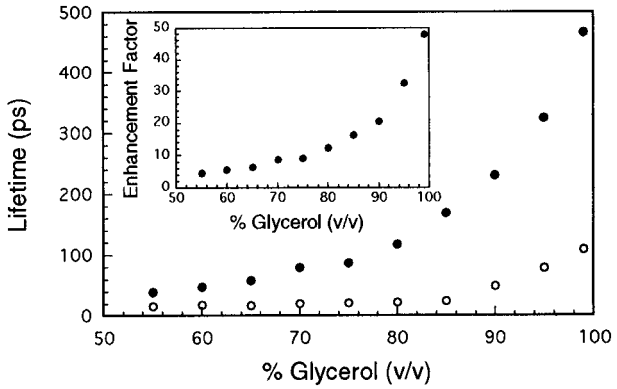


**Figure 3.** Fluorescence lifetimes of TNP-ATP in glycerol/water mixtures as a function of the glycerol percentage (v/v). The longer and shorter time constants of the biexponential fit are indicated by the dots and open circles, respectively. The inset shows the enhancement factors of fluorescence intensity compared with the fluorescence of TNP-ATP in pure water.

This function is written as

$$I(t) = A \exp\left[-\left(\frac{t}{\tau}\right)^{\beta}\right] \tag{1}$$

where $I(t)$ represents the fluorescence intensity, $A$ is a preexponential factor, $\tau$ is a characteristic time constant, and $\beta$ is the width of the distribution of time constants and has a range from 0 to 1. For $\beta = 1$, eq 1 is reduced to a single exponential. In the least-squares fitting process with the stretched exponential function, we included the instrument-response function in the deconvolution. The fitted curve (dashed line in Figure 2) systematically deviates from the data in the long-time region, and results in the reduced $\chi^2$ value as large as 10.67. It has been suggested that acceptable reduced $\chi^2$ values range from 0.8 to 1.2.[31] Such a poor fitting with the stretched exponential function indicates that the nonexponential curve is not well-represented by a series of exponential functions with a distribution of time constants around only one characteristic value.

For the second trial, we fit the data by using the following biexponential function:

$$I(t) = A_1 \exp\left(-\frac{t}{\tau_1}\right) + A_2 \exp\left(-\frac{t}{\tau_2}\right) \tag{2}$$

with two time constants $\tau_1$ and $\tau_2$, and preexponential factors $A_1$ and $A_2$. The reduced $\chi^2$ value of the fitting (solid line in Figure 2) is 1.13, which indicates an acceptable fit. Although the biexponential fitting does not necessarily indicate that the decay curve has only two discrete time constants, it may imply a distribution of time constants around two well-separated values. The two time constants obtained here represent the characteristic time scales of two relaxation processes.

We obtained the fluorescence lifetime as a function of the percentage of glycerol (Figure 3). Comparison of the total fluorescence photocounts of TNP-ATP in glycerol/water mixtures with those of TNP-ATP at the same concentration in pure water (inset in Figure 3) shows that the fluorescence was enhanced with increasing viscosity, a result that agrees with previous steady-state measurements.[5] The fluorescence lifetime increased with increasing viscosity in a manner similar to that of the enhancement factor, therefore, so does the fluorescence quantum yield. This behavior indicates that the increase in fluorescence intensity with increasing viscosity results from the change in fluorescence lifetime and quantum yield.

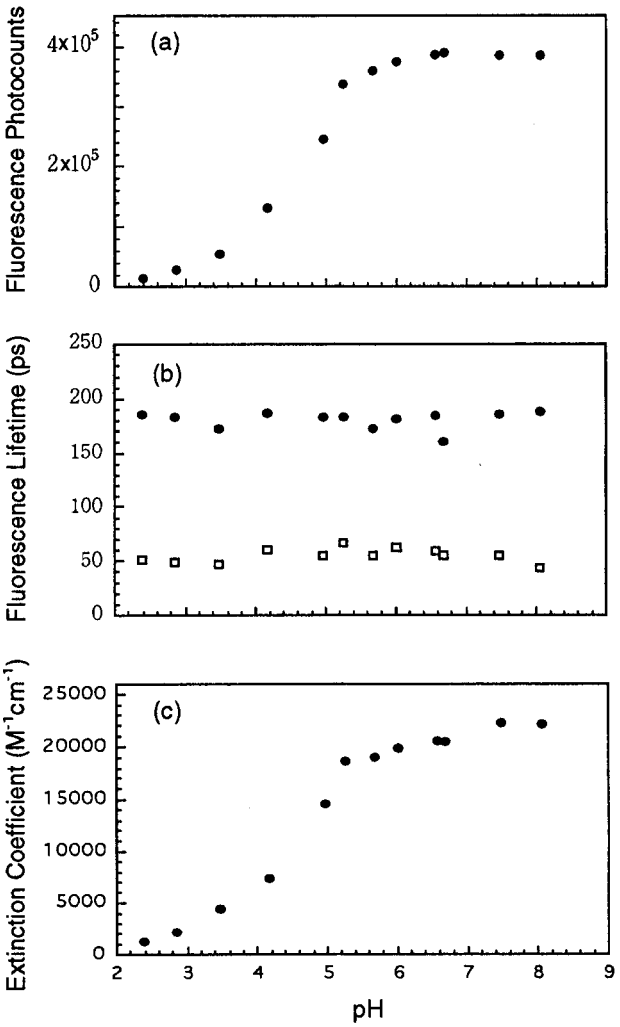


**Figure 4.** pH dependence of the spectroscopic properties of TNP-ATP in 87% (v/v) glycerol/water mixture: (a) total fluorescence photocounts; (b) two time constants of fluorescence decay obtained by least-squares fitting with biexponential functions (dots show the longer time constant, and squares the shorter); (c) molar extinction coefficient at 400 nm.

**Effect of pH on the Spectroscopic Properties of TNP-ATP.** The pH level is one of the most important factors of a biological system. We therefore investigated the effect of pH on the spectroscopic properties of TNP-ATP in glycerol/water mixtures of fixed composition. The fluorescence intensity increased with increasing pH (Figure 4a) and reached a saturated value at neutral and basic pH. These results are consistent with previous measurements.[5] The fact that the fluorescence has maximal intensity in the physiological pH range makes TNP-ATP suitable for the study of its interaction with proteins.

To determine the origin of the pH dependence of the fluorescence intensity, we used time-resolved fluorescence measurements and found that the fluorescence spectra (not shown here) and lifetimes (Figure 4b) were essentially independent of pH. This independence indicates that the pH dependence of fluorescence intensity is not due to the change in fluorescence lifetime and quantum yield. This finding is in sharp contrast to the viscosity dependence of fluorescence intensity, as discussed in the previous section. We also measured the absorption spectra of TNP-ATP in solvents with different pH. The molar extinction coefficient at 400-nm excitation varied with pH (Figure 4c) in a manner similar to that of the fluorescence intensity. As illustrated by previous studies,[5,32] a change in absorbance is characteristic of a Meisenheimer complex and was attributed to the pH-induced change in equilibrium between two species of TNP-ATP. At acidic pH the possibility increases for opening the dioxolane ring of TNP-ATP at the 2′-oxygen to yield 3′-*O*-(trinitrophenyl) adenosine 5′-triphosphate, which has absorption in the ultraviolet region but not in the visible region. The variation in the absorption spectrum induced by the formation of a different TNP-ATP species leads to the pH dependence of fluorescence intensity. The pH independence of the fluorescence spectrum and lifetime revealed by the time-resolved fluorescence measurement suggests that only the species of TNP-ATP with the Meisenheimer complex is responsible for the observed fluorescence.

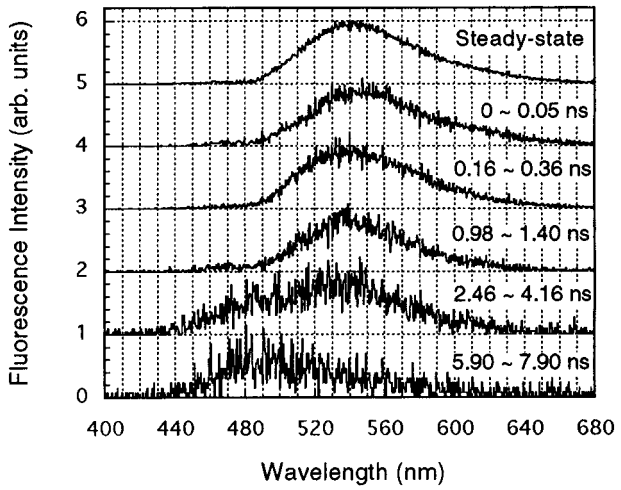


**Figure 5.** Time-resolved fluorescence spectra of TNP-ATP (6.0 $\mu$M) in the presence of the Klenow fragment (3.5 $\mu$M) in 0.2 M Tris−HCl (pH 8.0). The steady-state spectrum is also shown for comparison. All spectra were normalized to unity at their maximum and shifted vertically by one unit with respect to each other.

**Interaction of TNP-ATP with the Klenow Fragment of Pol I.** Much attention has been focused on the study of the Klenow fragment,[8,33] a multifunctional enzyme, which is involved in the repair and replication of DNA in *Escherichia coli*. TNP-ATP has also been used as a fluorescent probe to study the binding nature of this enzyme.[8] An increase in fluorescence intensity by titrations of the enzyme with TNP-ATP was previously observed by using steady-state measurements. In the present study, we have used time-resolved spectroscopy to provide a more detailed view of the interaction between the enzyme and TNP-ATP. By using a sufficiently long time scale of observation (10 ns), we observed most relaxation processes of interest. Figure 5 shows the time-resolved fluorescence spectra for TNP-ATP (6.0 $\mu$M) mixed with the Klenow fragment (3.5 $\mu$M) in 0.2 M Tris−HCl (pH 8.0). The steady-state spectrum was plotted in the upper recording of Figure 5 for comparison. In the long-time decay region, the time-resolved measurements resolved a weak fluorescence band with an emission peak at ∼490 nm well-separated from the main fluorescence emission peak around 540 nm. We estimated that the weak fluorescence was 2 orders of magnitude weaker than that of the main fluorescence band. Such a weak fluorescence band was blurred in the steady-state spectrum and therefore previously remained undetected. In a given region of time, for instance from 2.46 to 4.16 ns, the two fluorescence bands had comparable amplitudes (Figure 5). Another two curves plotted in this figure corresponding to 0.16−0.36- and 0.98−1.40-ns regions represent the spectra of the main fluorescence band, where little time-resolved spectrum shift occurs. This negligible shift implies that solvation plays a less important role in this

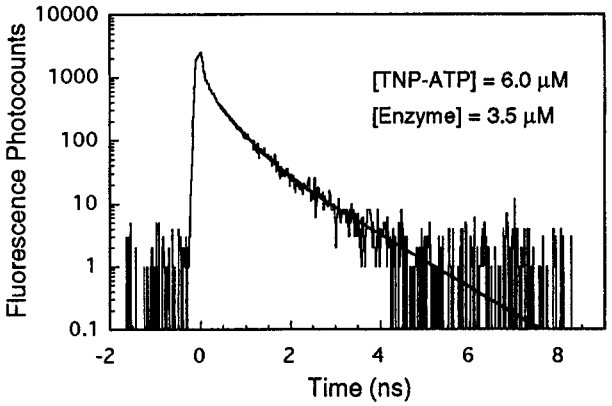


**Figure 6.** Fluorescence decay curve of TNP-ATP (6.0 $\mu$M) in the presence of the Klenow fragment (3.5 $\mu$M) in 0.2 M Tris−HCl (pH 8.0) determined over the 560- to 640-nm wavelength range. An extremely fast decay appears in the initial time region to a nonzero level followed by a long decay tail.

sample than in the sample of TNP-ATP in glycerol/water mixtures. The spectrum related to the initial decay had an emission peak of longer wavelength than the spectra in later time regions. Next we discuss the assignment of these spectra.

The fluorescence decay curve for TNP-ATP with the Klenow fragment (Figure 6) was determined over the wavelength range from 560 to 640 nm rather than the entire wavelength range to eliminate the intervention of the long-lived component to the decay curve with respect to the main fluorescence band. The profile for this curve is notably different from that for the decay curve for TNP-ATP in a glycerol/water mixture (Figure 2). A sharp peak occurred in the initial decay region, followed by a long tail. The fast component decayed too rapidly to be resolved with the detection system even when we used the shortest time scale (1 ns) to improve the time resolution to less than 22 ps. This fast decay component may arise from the fluorescence of free TNP-ATP in the solution, whereas the long fluorescence tail may come from the TNP-ATP bound to the enzyme. This attribution is also supported by the finding that the spectrum for the initial decay time is different from the spectra in the subsequent time (Figure 5).

The long decay tail is well fitted to a biexponential function with a reduced $\chi^2$ value of 1.05. The time constants of the biexponential fitting were essentially independent of the enzyme concentration (Figure 7a). This independence suggests that this long decay tail is common to all of the samples with the Klenow fragment and supports the assignment of this decay component to the bound TNP-ATP. The amplitudes of the decay components increased with increasing enzyme concentration (Figure 7b), although the lifetime was essentially independent. This implies an increase in the number of bound molecules and reveals that the main reason for the increase in total fluorescence photocounts with increasing enzyme concentration (Figure 8) is due to the increase in the amplitude of the slow decay components, but not to the change in fluorescence lifetime.

To obtain the corresponding fluorescence lifetime of the weak fluorescence band, we take the decay curve over the wavelength range from 440 to 500 nm away from the strong fluorescence band to manifest this weak decay component. We estimated the lifetime of the long-lived decay component to be 4.1 ns. This extremely slow decay component may arise from a binding site distinct from the dominant binding site. The affinity of TNP-ATP to this site is much lower than that to the dominant site, although the fluorescence lifetime of TNP-ATP bound to this site is longer than that bound to the dominant site. Note that

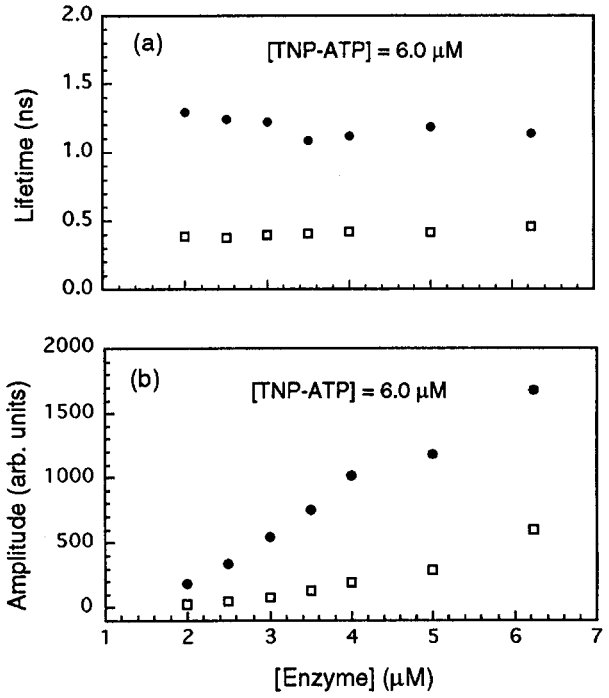


**Figure 7.** Fluorescence titration of TNP-ATP (6.0 $\mu$M) with the Klenow fragment in 0.2 M Tris−HCl (pH 8.0). (a) Fluorescence lifetime and (b) amplitudes of the main fluorescence band of bound TNP-ATP are shown as functions of the enzyme concentration. The dots and squares represent the values corresponding to the slow and fast decay components of the biexponential fitting, respectively.

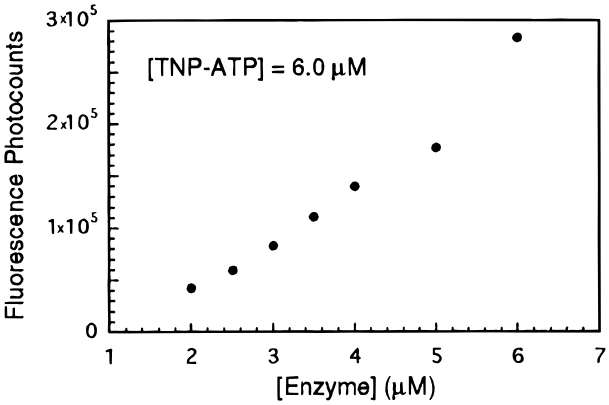


**Figure 8.** Total fluorescence photocounts of TNP-ATP (6.0 $\mu$M) as a function of the Klenow-fragment concentration.

the binding site with lower affinity could not be resolved in previous steady-state measurements.

As we discussed earlier in this section, the blue-shifted time-resolved spectra of TNP-ATP with the Klenow fragment (Figure 5) result from the fluorescence of three origins with different emission spectra and lifetimes. This contrasts with the TNP-ATP in glycerol/water mixture where the red-shift of time-resolved spectra is caused by the solvation effect.

**Effect of $Mg^{2+}$ on the Binding of TNP-ATP with the Klenow Fragment.** The addition of $Mg^{2+}$ enhanced the fluorescence intensity of TNP-ATP in the presence of the Klenow fragment by 1.5-fold. Control experiments in the absence of the enzyme showed no such $Mg^{2+}$-induced enhancement in the fluorescence of TNP-ATP. The fluorescence decay curves of TNP-ATP in the presence of enzyme with and without $Mg^{2+}$ (Figure 9) show that the amplitude of the slow decay component was increased by the addition of $Mg^{2+}$, whereas the fluorescence lifetime remained almost unchanged. As discussed

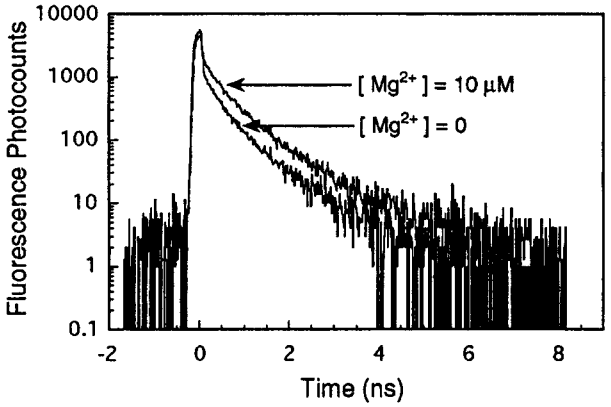


**Figure 9.** Fluorescence decay curves of TNP-ATP (10 $\mu$M) in the presence of the Klenow fragment (4.0 $\mu$M) in 0.2 M Tris−HCl (pH 8.0) with and without $Mg^{2+}$.

in the previous section, the increase in amplitude of the slow decay component indicates an increase in the number of bound TNP-ATP molecules. Because the fluorescence from bound TNP-ATP has a longer lifetime, and therefore higher quantum yield than that from free TNP-ATP, the total fluorescence photocounts increase when the number of bound TNP-ATP is increased by the addition of $Mg^{2+}$. This result suggests that $Mg^{2+}$ increases the affinity of the enzyme for TNP-ATP. This conclusion is different from the one drawn from steady-state measurements, that the presence of $Mg^{2+}$ does not alter the affinity of the enzyme for TNP-ATP but that the enzyme raises the affinity of TNP-ATP for $Mg^{2+}$.[8] The present time-resolved fluorescence measurement is straightforward and gives a direct measurement of the binding nature. The experimental evidence in Figure 9 is clear, and therefore the conclusion based on the time-resolved measurements is more reliable than that based on previous steady-state measurements.

## IV. Conclusions

We used time-resolved fluorescence spectroscopy to investigate the transient fluorescence properties of the nucleotide analogue TNP-ATP in various solvents. The results show that the time-resolved fluorescence spectra red-shift for TNP-ATP in glycerol/water mixtures is attributed to the solvation effect, whereas the observed blue-shift for TNP-ATP in the presence of the Klenow fragment is ascribed to the overlap of fluorescence spectra from free TNP-ATP and bound TNP-ATP from two different binding sites. Our results also illustrate the environmental dependence of the fluorescence lifetime. The increase in the fluorescence lifetime with increasing viscosity indicates that the enhancement of fluorescence intensity is due to the increase in fluorescence quantum yield. However, the fluorescence lifetime is unaffected by variations in pH, whereas the fluorescence intensity changes in a manner similar to that of the extinction coefficient when pH changes from acidic to basic values. Furthermore, the complicated nature of the fluorescence of TNP-ATP in the presence of an enzyme was revealed in both the frequency and time domains. The fluorescence from the enzyme−TNP-ATP complex had two emission bands with different decay-time constants, suggesting that there are two binding sites of the enzyme for TNP-ATP. The binding site with lower affinity could not be resolved in previous steady-state measurements. The fluorescence from free TNP-ATP had a longer wavelength emission and appeared as a time-resolution-limited decay in the fluorescence decay curve. The fluorescence lifetime of bound TNP-ATP was independent of titrations with the enzyme, whereas the amplitude of this fluorescence component increased with increasing enzyme concentration, thus increasing the fluorescence intensity. Moreover, the increase in the amplitude of the slow decay component by the addition of $Mg^{2+}$ indicates that $Mg^{2+}$ increases the affinity of enzyme for TNP-ATP.

The present time-resolved spectroscopy shows that the spectroscopic properties of TNP-ATP are extremely sensitive to local environments and provides an in-depth view of the origins for the enhancement of fluorescence intensity, which were obscured in previous steady-state measurements. This study suggests that time-resolved spectroscopy is much more informative than steady-state measurements. Further experiments on the enhanced fluorescence of TNP-ATP with single-molecule detection are planned soon and may provide further insight into individual molecules.

**Acknowledgment.** This work was performed at JRCAT under the management of ATP, and partly supported by the New Energy and Industrial Technology Development Organization of Japan (NEDO). We are indebted to Drs. Kazuo Umemura, Naoaki Okamoto, and Minoru Takeuchi for helpful discussions.

## References and Notes

(1) Secrist, J. A.; Barrio, J. R.; Leonard, N. J. *Science* **1972**, *175*, 646.
(2) Leonard, N. J.; Scopes, D. I. C.; VanDerLijn, P.; Barrio, J. R. *Biochemistry* **1978**, *17*, 3677.
(3) Ward, D. C.; Reich, E.; Stryer, L. *J. Biol. Chem.* **1969**, *244*, 1228.
(4) Hiratsuka, T.; Uchida, K. *Biochim. Biophys. Acta* **1973**, *320*, 635.
(5) Hiratsuka, T. *Biochim. Biophys. Acta* **1976**, *453*, 293; **1982**, *719*, 509.
(6) Rai, S. S.; Kasturi, S. R. *Biophys. Chem.* **1994**, *48*, 359.
(7) Moczydlowski, E. G.; Fortes, P. A. G. *J. Biol. Chem.* **1981**, *256*, 2346.
(8) Mullen, G. P.; Shenbagamurthi, P.; Mildvan, A. S. *J. Biol. Chem.* **1989**, *264*, 19637.
(9) Liu, R.; Sharom, F. J. *Biochemistry* **1997**, *36*, 2836.
(10) Weber, J.; Senior, A. E. *FEBS Lett.* **1997**, *412*, 169.
(11) Broglie, K. E.; Takahashi, M. *J. Biol. Chem.* **1983**, *258*, 12940.
(12) Bandorowicz-Pikula, J. *Mol. Cell. Biochem.* **1998**, *181*, 11.
(13) Gatto, C.; Wang, A. X.; Kaplan, J. H. *J. Biol. Chem.* **1998**, *273*, 10578.
(14) Neville, D. C. A.; Rozanas, C. R.; Tulk, B. M.; Townsend, R. R.; Verkman, A. S. *Biochemistry* **1998**, *37*, 2401.
(15) Mockett, B. G.; Housley, G. D.; Thorne, P. R. *J. Neurosci*. **1994**, *14*, 6992.
(16) Weber J.; Senior, A. E. *J. Biol. Chem.* **1996**, *271*, 3474.
(17) Lin, S. H.; Faller, L. D. *Biochemistry* **1996**, *35*, 8419.
(18) Gabellier, E.; Strambini, G. B.; Baracca, A.; Solaini, G. *Biophys. J.* **1997**, *72*, 1818.
(19) Smyczynski, C.; Kasprzak, A. A. *Biochemistry* **1997**, *36*, 13201.
(20) Miki, M.; Miura, T.; Sano, K.; Kimura, H.; Kondo, H.; Ishida, H.; Maeda, Y. *J. Biochem.* **1998**, *123*, 1104.
(21) Ye, J. Y.; Hattori, T.; Inouye, H.; Ueta, H.; Nakatsuka, H.; Maruyama, Y.; Ishikawa, M. *Phys. Rev. B* **1996**, *53*, 8349; Ye, J. Y.; Hattori, T.; Nakatsuka, H.; Maruyama, Y.; Ishikawa, M. *ibid.* **1997**, *56*, 5286.
(22) Ye, J. Y.; Ishikawa, M.; Yogi, O.; Okada, T.; Maruyama, Y. *Chem. Phys. Lett.* **1998**, *288*, 885.
(23) Abedin, K. M.; Ye, J. Y.; Inouye, H.; Hattori, T.; Sumi, H.; Nakatsuka, H. *J. Chem. Phys.* **1995**, *103*, 6414.
(24) Ishikawa, M.; Watanabe, M.; Hayakawa, T.; Koishi, M. *Anal. Chem.* **1995**, *67*, 551.
(25) Simon, J. D. *Acc. Chem. Res.* **1988**, *21*, 128.
(26) Fried, L. E.; Mukamel, S. *J. Chem. Phys.* **1990**, *93*, 932.
(27) Fourkas, J. T.; Berg, M. *J. Chem. Phys.* **1993**, *98*, 7773.
(28) Argaman, R.; Huppert, D. *J. Phys. Chem. A* **1998**, *102*, 6215.
(29) Pratap, P. R.; Hellen, E. H.; Palit, A.; Robinson, J. D. *Biophys. Chem.* **1997**, *69*, 137.
(30) Sidebottom, D. L.; Bergman, R.; Borjesson, L.; Torell, L. M. *Phys. Rev. Lett.* **1992**, *68*, 3587.
(31) O'Conner, D. V.; Phillips, D. *Time-correlated Single Photon Counting*; Academic Press: London, 1984; pp 181−182.
(32) Strauss, M. J. *Chem. Rev.* **1970**, *70*, 667.
(33) Guest, C. R.; Hochstrasser, R. A.; Dupuy, C. G.; Allen, D. J.; Benkovic, S. J.; Millar, D. P. *Biochemistry* **1991**, *30*, 8759.